XA9540808

221

RESIDUAL AND OPERATING STRESSES IN WELDED ALLOY 600 PENETRATIONS

E. Stephen Hunt*, David J. Gross*, Raj Pathania**
* Dominion Engineering, Inc., 6862 Elm St., McLean, VA, 22101, USA
**EPRI, 3412 Hillview Avenue, Palo Alto, CA, 94303, USA

ABSTRACT

An elastic-plastic finite element model has been developed for calculating residual and operating stresses in Alloy 600 penetrations which are installed in pressure vessel shells by J-groove welds. The welding process is simulated by multiple passes of heat input with heat transfer into the adjacent parts during welding and cooling.

Analysis results are presented for CRDM nozzles, pressurizer instrument nozzles and pressurizer heater sleeves. The effect of several key variables such as nozzle material yield strength, angle of the nozzle relative to the vessel shell, weld size, presence of counterbores, etc. are explored. Results of the modeling are correlated with field and laboratory data. Application of the stress analysis results to PWSCC predictive modeling is discussed.

1. INTRODUCTION

Primary water stress corrosion cracking (PWSCC) of Alloy 600 primary loop penetrations in PWR plants was first reported in 1982 in a pressurizer heater sleeve at Arkansas Nuclear One Unit 2. PWSCC has subsequently been reported in several other types of primary loop penetrations in PWR plants including pressurizer instrument nozzles, steam generator drains, and reactor vessel head CRDM nozzles (1). Figure 1 shows typical penetration arrangements and crack locations. It is noted that the cracks in all of the penetrations are located near the J-groove welds which attach the penetrations to the vessel shells.

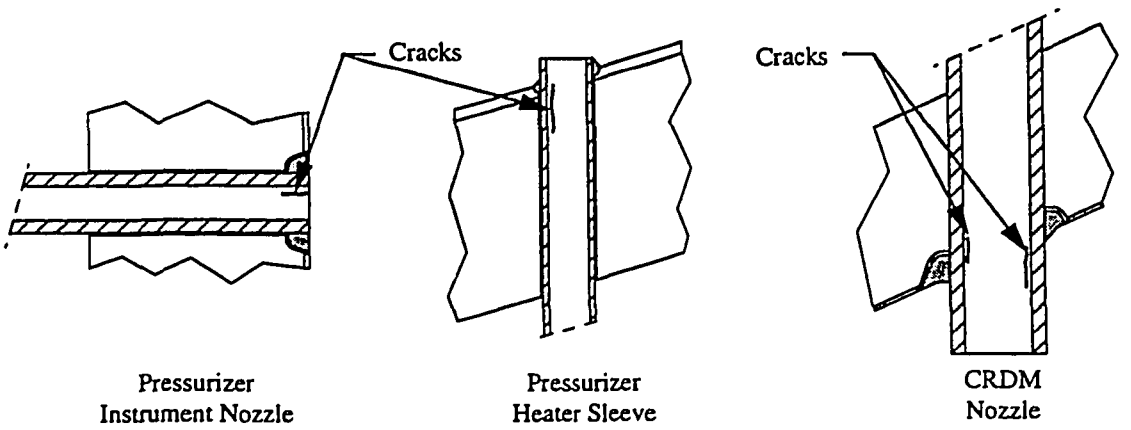

Figure 1– Typical Alloy 600 Penetrations and Crack Locations

Tensile stresses are necessary for PWSCC to occur in Alloy 600 materials. Tensile stresses can be induced by internal pressure and differential thermal expansion under operating conditions. However, these stresses are limited by design code requirements and the stresses generally do not exceed 100–200 MPa. These pressure and thermal stresses are less than the stress threshold for PWSCC of Alloy 600 material in normal PWR environments. However, much higher tensile stresses can be created by shrinkage forces when penetrations are welded into vessel shells. The combination of operating stresses superimposed on high residual stresses produced by welding is believed to be a major contributing cause of the PWSCC which has been reported in Alloy 600 PWR penetrations.

2. ANALYSIS METHOD

Stresses in CRDM nozzles, pressurizer instrument nozzles and pressurizer heater sleeves have been calculated using the elastic-plastic finite element method and the ANSYS finite element analysis program. All nozzles are analyzed as 3D penetrations in spherical shells. As shown in Figures 2 and 3, the models include a conical sector of the vessel shell, and the boundary conditions are selected to permit only radial deflections in the spherical coordinate system. These boundary conditions simulate the stiffness and pressure stresses in the vessel shells remote from the penetrations.

Four materials are considered in the analyses. The vessel shells are assumed to be low alloy steel, the penetrations are assumed to be Alloy 600, the J-groove welds and buttering are assumed to be Inconel weld metal, and the cladding on the inside surfaces of the vessel shells is assumed to be either 300 series stainless steel, or Inconel as appropriate. Materials are assumed to have temperature dependent material properties. Figure 4 shows typical yield strengths of the materials as a function of temperature. High temperature properties for the Inconel materials were developed by EdF (2) based on work performed in their mockup testing program.

The analyses of the penetrations involved four loading steps:

Nozzle Installation – Pressurizer instrument nozzles and heater sleeves are installed in clearance holes in the vessel shells. The clearance holes are simulated in the finite element models by gap elements. CRDM nozzles are installed in the vessel heads using either a metal-to-metal fit or a small interference. CRDM nozzle analyses were all performed for the case of a metal-to-metal fit since separate effects studies showed that this condition produces the highest tensile stresses on the inside surface of the nozzles. Gap elements with zero initial clearance are used to simulate the metal-to-metal fit between the CRDM nozzles and holes in the vessel heads, and to permit some displacement of the nozzle wall as the pressure stresses in the vessel shell cause the hole to dilate.

Welding – All of the nozzles evaluated are joined to the vessel shells by J-groove welds. The J-groove welds are simulated as rings of weld metal in which one ring is applied at a time. Non-axisymmetric effects of progressively deposited welds are neglected. Parametric analyses showed that two weld passes provide a good approximation of the stress distributions on the inside surface of the nozzles predicted using larger numbers of passes. The welding process is simulated by combined thermal and structural analyses. Thermal analyses are used to generate temperature distributions throughout the joint at several points in time during the welding process. These temperature distributions are then used as input conditions to the structural analyses. The sequence of thermal analyses followed by structural analyses was duplicated for each of the two simulated welding passes. Figure 5 shows the temperature distribution during the first pass of a typical CRDM nozzle weld.

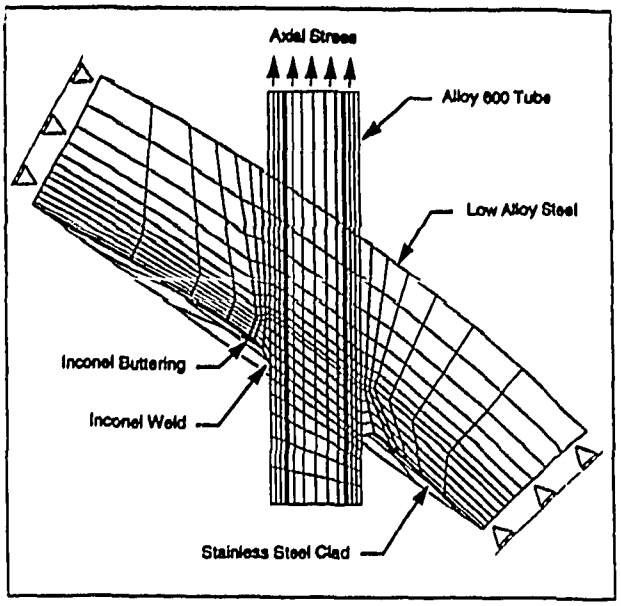

Figure 2 – Finite Element Model of Typical CRDM Nozzle

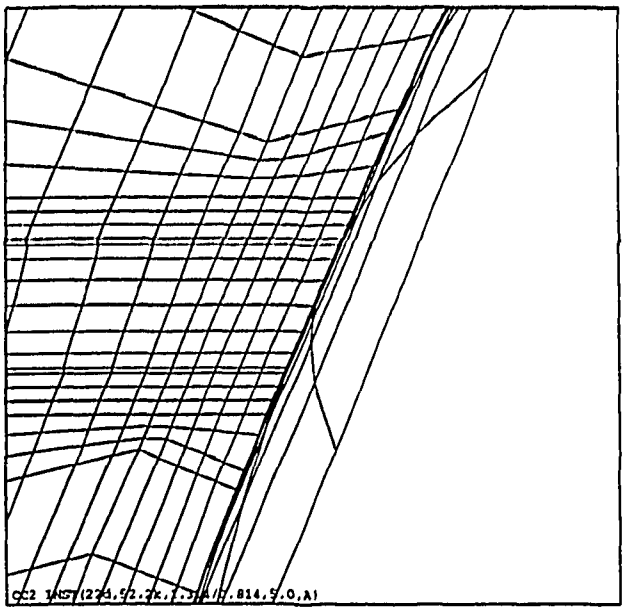

Figure 3 – Finite Element Model of Typical Pressurizer Instrument Nozzle

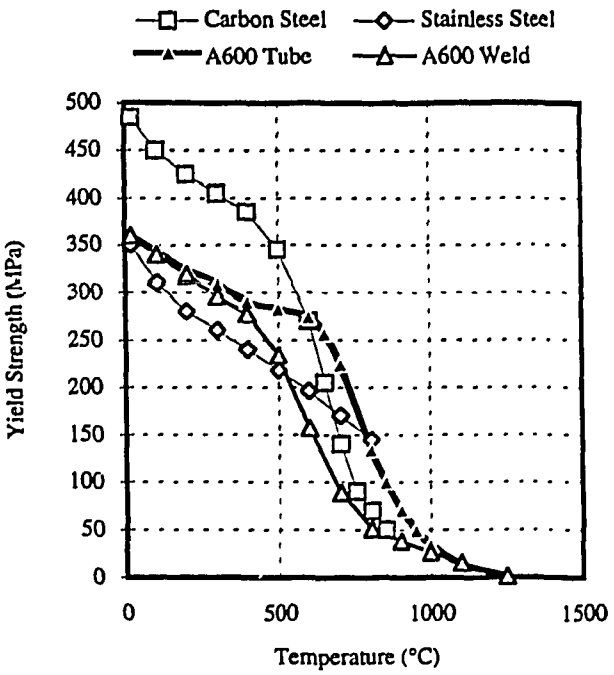

Figure 4 – Typical High Temperature Yield Strengths

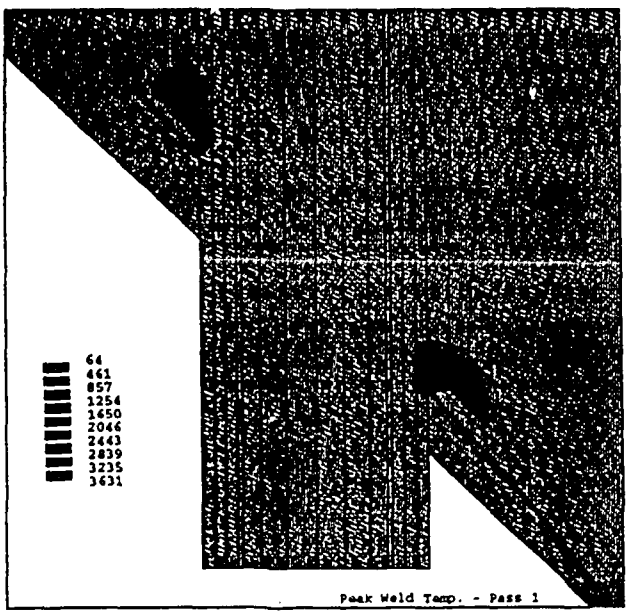

Figure 5 – Typical First Pass Weld Temperature Distribution

Hydrostatic Testing – The pressure vessels and nozzles are hydrostatically tested to a pressure of about 215 bar prior to plant operation. This operation is simulated by applying an internal pressure to the inside surface of the vessel shell and nozzle and an axial load on the end of the nozzle.

Operating Conditions – The final loading step is to apply an internal pressure of 155 bar, a uniform temperature of 315°C, and an axial load on the end of the nozzle.

3. ANALYSIS CASES AND RESULTS

Analyses have been performed for a wide range of different penetration and mockup designs. Several cases of general interest and key analysis results are given in Table 1.

Figure 6 shows the deformed shape of typical central and outer row CRDM nozzles after welding (Note: The displacement scales are exaggerated.) The weld metal is not shown in these figures since it is highly distorted at the selected scale. The figure of the central nozzle shows the nozzle wall being pulled radially outward by the weld shrinkage. This deflection produces high tensile hoop stresses and somewhat lower axial stresses. The figure of the outer nozzle shows that the bottom of the nozzle is deflected laterally away from the center of the vessel head and that the nozzle becomes ovalized by weld shrinkage.

Figure 7 is a plot of the hoop stresses along the inside surface of a typical outer row CRDM nozzle on the downhill side of the nozzle (side farthest from the center of the vessel head). This figure shows high residual stresses after welding, reduced residual stresses after a cold hydrostatic test, and operating condition stresses between these two extremes. This figure shows the beneficial effect of hydrostatic testing in reducing residual stresses. The cause of the stress reduction is as follows: 1) maximum stresses in the nozzle wall are close to the material yield strength after welding, 2) the pressure induced dilation of the vessel head causes yielding of the portion of the nozzle near the weld, and 3) the material relaxes to a residual stress less than the material yield strength after the internal pressure is removed. The absence of a hydrostatic test after replacing some pressurizer nozzles may have contributed to the replacement nozzles developing through-wall cracks in a shorter time than the original nozzles.

Figure 8 shows the hoop and axial stresses along the inside surface of a typical outer row CRDM nozzle. These data show that the hoop stresses exceed the axial stresses at all high stress locations. This fact is confirmed by the data in Table 1 for several other nozzle configurations and locations.

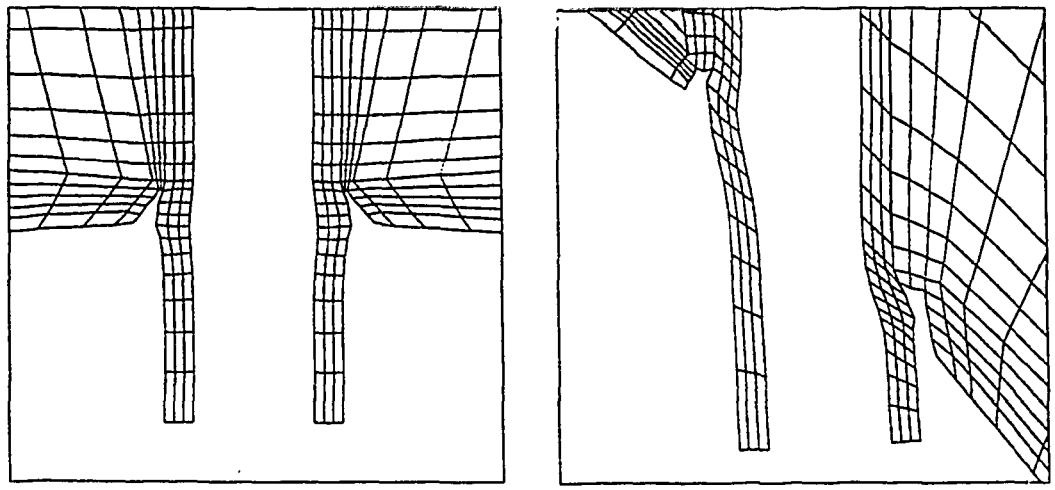

Figure 6 – Deflections After Welding in Typical Central and Outer Row CRDM Nozzles

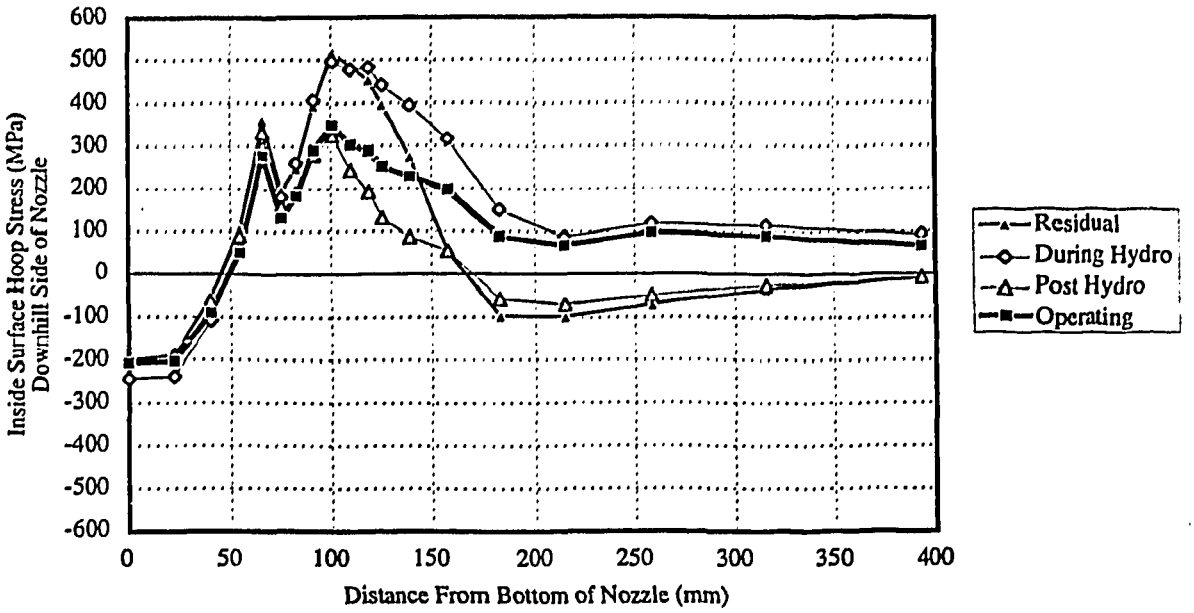

Figure 7 – Hoop Stress on Inside Surface of Typical Outer Row CRDM Nozzle

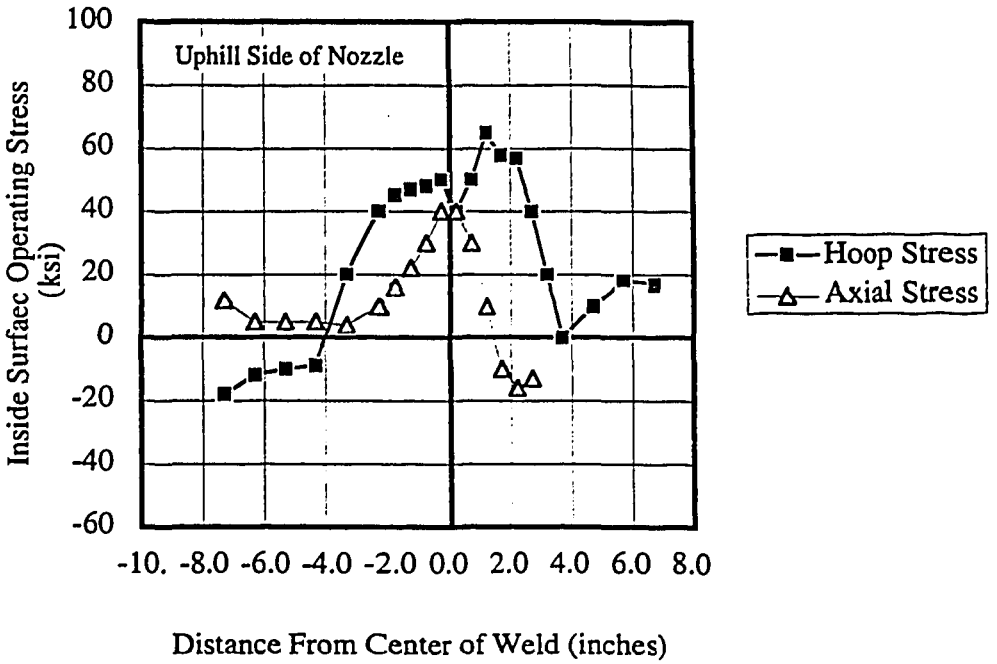

Figure 8 – Operating Hoop and Axial Stresses on Inside Surface of Typical Outer Row CRDM Nozzle

Table 1 Analysis Cases and Selected Results

Parameter	Units	Pressurizer Nozzles			EdF CRDM Nozzles*				
		Instrument	Heater Sleeve		Central	Intermediate Row		Outer Row	
Counterbore on Nozzle Inside Surface	---	No	No	No	No	No	Cylind	No	Taper
Material Yield Strength	MPa	359	359	435	359	359	359	359	359
Nozzle Incidence Angle	deg	22.5	45	45	0	39	39	47	47
Nozzle Geometry									
– Nozzle Outside Diameter, OD	mm	33.4	29.4	29.4	101.6	101.6	101.6	101.6	101.6
– Nozzle Inside Diameter, ID	mm	20.7	23.2	23.2	69.9	69.9	69.9	69.9	69.9
– Nozzle Wall Thickness, t	mm	6.4	3.1	3.1	15.9	15.9	15.9	15.9	15.9
– OD/t	---	5.26	9.51	9.51	6.40	6.40	6.40	6.40	6.40
MaxID Surface Deflections (Residual)									
– Diametral Increase	mm	---	---	---	0.28	---	---	---	---
– Lateral Deflection	mm	---	---	---	---	0.66	0.66	0.97	0.97
– Ovality	mm	---	---	---	---	0.89	0.84	1.19	1.32
Max ID Hoop Stresses (Operating)									
– Axisymmetric Nozzles	MPa	---	---	---	302	---	---	---	---
– Oblique Nozzles – Uphill	MPa	401	423	497	---	396	395	384	381
– Oblique Nozzles – Downhill	MPa	408	358	410	---	280	298	308	348
Max ID Axial Stresses (Operating)									
– Axisymmetric Nozzles	MPa	---	---	---	239	---	---	---	---
– Oblique Nozzles – Uphill	MPa	264	341	399	---	331	331	329	324
– Oblique Nozzles – Downhill	MPa	333	239	270	---	220	230	219	258
Ratio of Axial Stresses to Hoop Stresses									
- Axisymmetric Nozzles	---	---	---	---	0.79	---	---	---	---
– Oblique Nozzles – Uphill	---	0.66	0.81	0.80	---	0.84	0.84	0.86	0.85
– Oblique Nozzles – Downhill	---	0.82	0.67	0.66	---	0.79	0.77	0.71	0.74

* Dimensions of EdF nozzles taken from EdF specification (2).

4. CORRELATION WITH FIELD AND EXPERIMENTAL DATA

Results of the finite element analyses have been correlated with available experimental and field data. These correlations are described in a recent EPRI summary report on Alloy 600 PWSCC (1). Key conclusions are as follows:

Correlations With Reported Crack Locations and Orientations – There is good correlation between the locations of high calculated tensile stresses in each nozzle type and the locations of reported cracking from the field.

- Cracking reported in the field has typically been located near the welds. Analyses show that the maximum stresses for all nozzle designs are located near the welds at locations correlating with the reported cracking.

- Cracking on the inside surfaces of CRDM and pressurizer nozzles has been predominantly axial. The only exceptions for plants with normal water chemistry have been shallow non-axial fissures in a few nozzles which have many predominantly axial fissures, and shallow circumferential cracks in roll expanded EdF pressurizer instrument nozzles. This experience is consistent with analysis results which show that the hoop stresses exceed the axial stresses at all high stress locations.

- Cracking in oblique CRDM nozzles has been axial and located on the uphill and downhill sides of the nozzles. The analyses show that the hoop stresses in oblique nozzles are highest on the uphill and downhill sides of the nozzles. High stresses at these locations result from ovality induced by weld shrinkage.

- Cracking in oblique nozzles has occurred predominantly below the welds on the uphill sides of the nozzles. Analyses for most outer row CRDM nozzles show that the maximum hoop stresses are typically highest below the weld on the uphill sides of the nozzles. However, this is not true in all cases. Figure 9 shows a plot of hoop stresses in Oconee 2 nozzle No. 23 and the very shallow indications which were found in this nozzle. Note that the indications are centered within the highest stress location, and that this location lies above the weld on the downhill side of the nozzle.

- Finally, cracking in CRDM nozzles occurs most frequently in the outer row nozzles. Analyses of typical central and outer row nozzles typically show that stresses are higher in the outer row nozzles. However, this is not always the case as discussed in Section 5.

Correlations With Measured Deflections – The maximum lateral deflection and ovality have been measured on several CRDM nozzle mockups. Table 2 provides a comparison of the measured and calculated deflections and ovality for mockups fabricated by EdF (2) and Ringhals (6). These results show that the measured and calculated deflections are in reasonably good agreement.

Table 2 – Comparison of Measured and Calculated Deflections and Ovalities

Mockup Design and Type of Deflection	Measured	Calculated
EdF CRDM Nozzle Mockup (47°)		
- Lateral Deflection (mm)	1.73	0.97
- Ovality (mm)	1.62	1.32
Ringhals CRDM Nozzle Mockup (43°)		
- Ovality (mm)	1.15	1.25

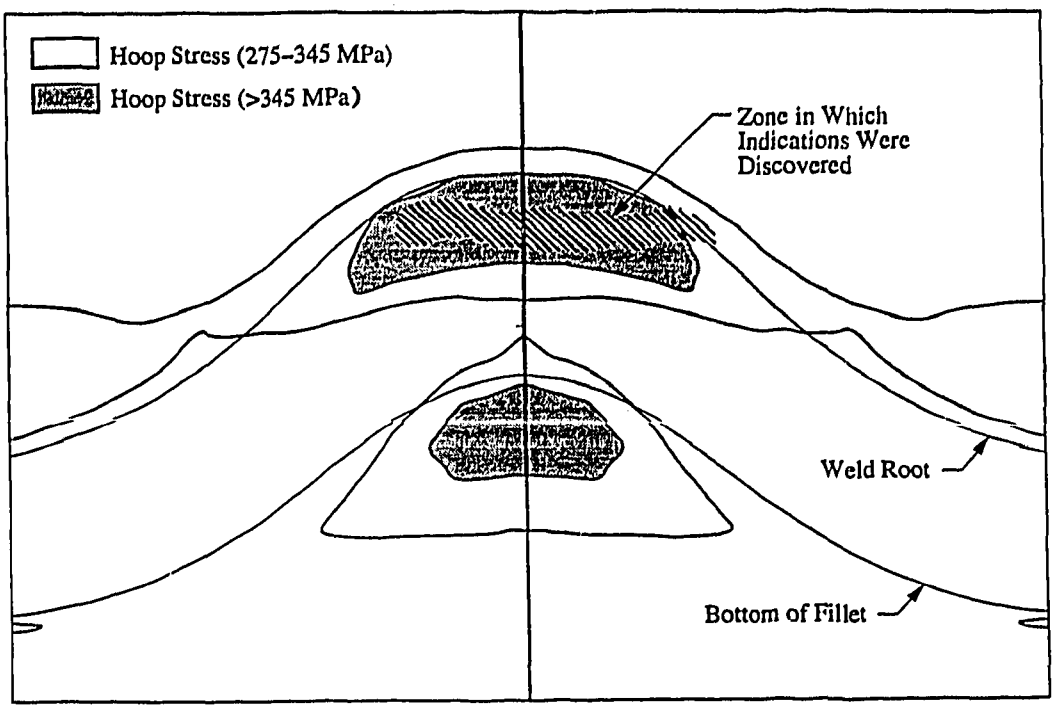

Figure 9 – Correlation Between High Stresses and Location of Axial Indications in Oconee 2 CRDM Nozzle No. 23

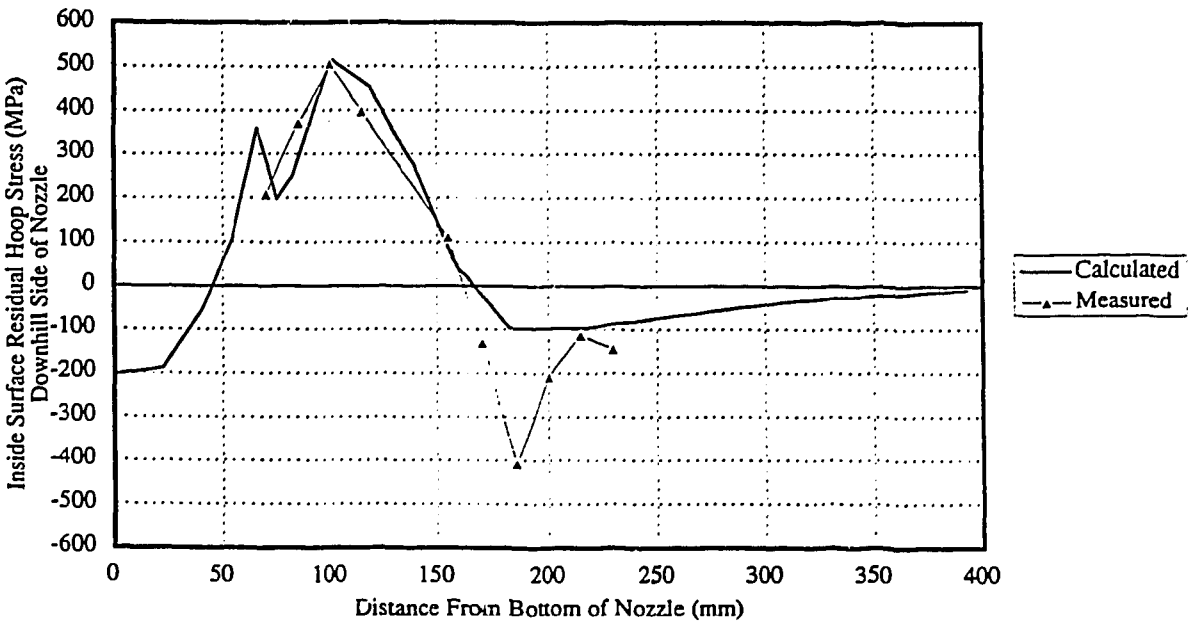

Figure 10 – Correlation Between Calculated and Measured Hoop Stresses in Typical Outer Row CRDM Nozzles

Correlations With Measured Residual Stresses – Combustion Engineering has performed x-ray residual stress measurements of pressurizer heater sleeve mockups for EPRI. A comparison of the experimental and analytical stress analyses is included in a recent EPRI report (5). The main conclusion from this work is that the analytical results provide an upper bound to the experimental results.

EdF has performed strain-gage hole drilling residual stress measurements on several CRDM nozzle mockups. Figure 10 shows that there is good agreement between the measured and calculated inside surface stresses for the downhill side of an outer row CRDM nozzle. More complete results are included in a recent EPRI report (1).

Comparison With Corrosion Test Experience – EdF and Framatome have performed corrosion tests on Alloy 600 CRDM nozzle mockups to determine crack orientation. The results of these tests showed that: (1) cracks occurred in outer row mockups but not in central mockups, (2) all cracks were axial, and (3) all cracks were located on the uphill and downhill sides of the nozzles. These findings are in agreement with the stress analysis results.

In summary, analysis results are considered to be in reasonably good agreement with reported field experience and laboratory testing.

5. EFFECT OF WELD DESIGN VARIATIONS ON STRESSES

A cursory review of drawings of CRDM nozzles from different vendors suggests that they are all essentially the same. On this basis it would be expected that all of the nozzles should have essentially the same maximum calculated stresses if analyzed using the same modeling assumptions, material properties, and computer program. In order to check this assumption analyses were performed for several different CRDM nozzle designs using the same assumptions, material properties and computer program described in Section 2 of this paper. The main differences between these nozzles were small differences in nozzle diameters and more significant differences in weld sizes.

Figure 11 shows the maximum hoop stresses in several different central CRDM nozzle designs as a function of the ratio of the length of the weld in contact with the nozzle to the nozzle wall thickness. The conclusion from this work is that the weld size is a significant variable in predicting the maximum operating condition stress.

Figure 12 shows the maximum inside surface hoop stresses in nozzles from several different plants for a range of nozzle incidence angles. These results were calculated assuming that all of the nozzles have a yield strength of 360 MPa. These data also show that weld size is a significant factor in predicting hoop stresses.

6. USE OF FINITE ELEMENT MODELING FOR STRATEGIC PLANNING

Work described in this paper has shown that there is a correlation between locations of high predicted tensile stresses and locations where cracking has been reported from the field. This information can be used in developing strategic plans to predict when cracks are likely to occur in a specific plant and which nozzles are likely to be affected by the cracking first. This information can be used by utilities to target inspections towards locations of highest predicted PWSCC susceptibility.

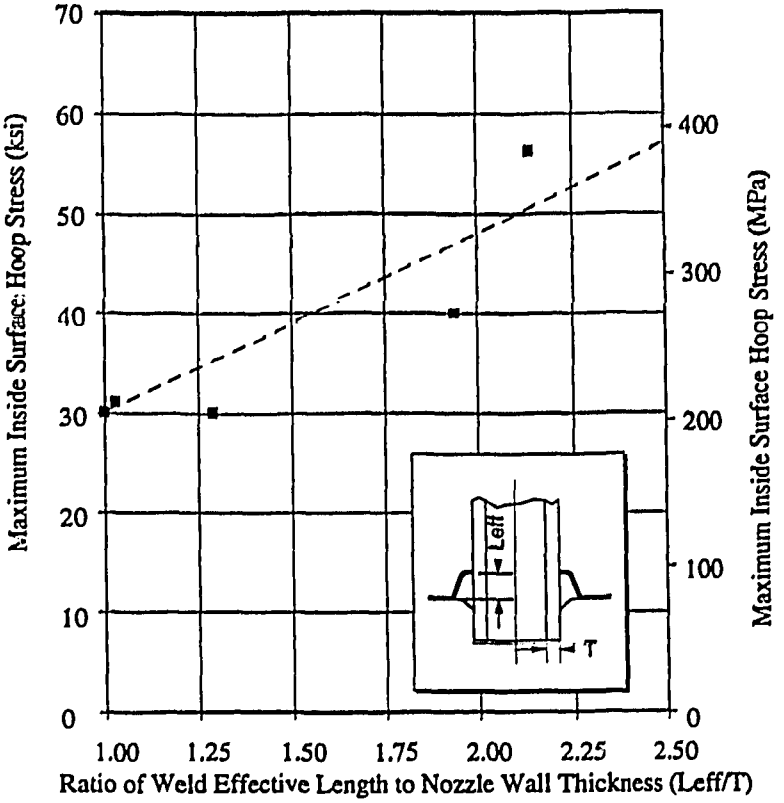

Figure 11 – Effect of Weld Size on Maximum Hoop Stress in Central CRDM Nozzles

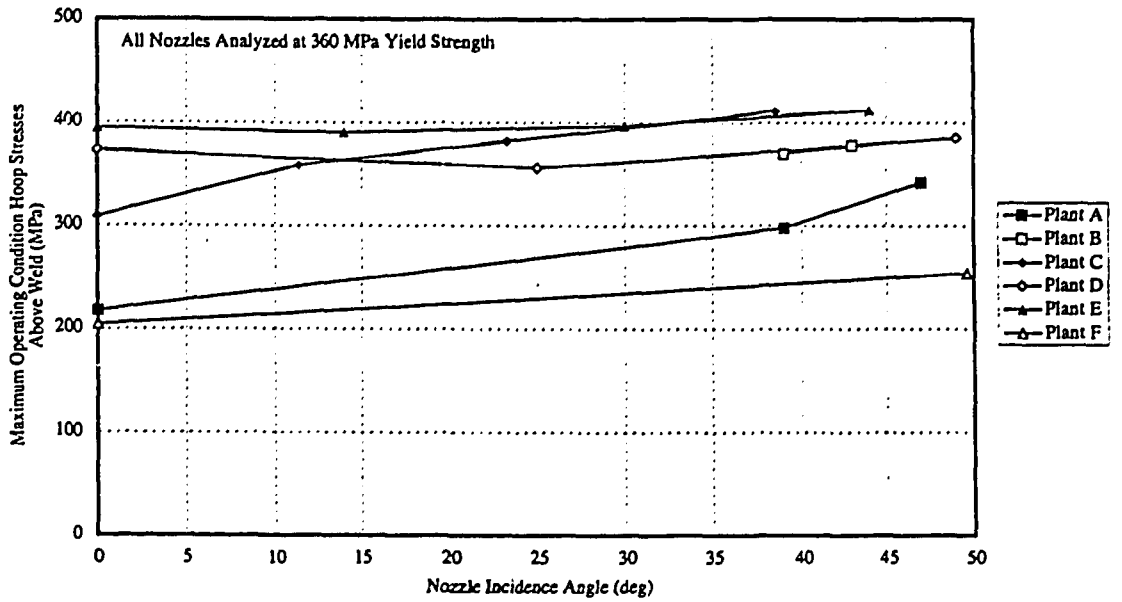

Figure 12 – Effect of Vessel Design on Hoop Stresses in CRDM Nozzles

7. CONCLUSIONS

The main conclusions from the finite element analysis work were as follows:

- The finite element method provides a reasonable approach for evaluating stress levels in welded nozzles.
- Welding a nozzle into a vessel shell with a J-groove weld produces a high restraint condition that can cause high tensile residual stresses.
- Weld heat input causes the nozzle wall to expand radially outward. Some of this thermal displacement is "locked-in" by the weld as it cools, contracts and strengthens.
- For outer row nozzles, the highest stresses are hoop stresses resulting from ovalization.
- Hoop stresses exceed axial stresses at all high stress locations such that cracking is expected to be predominantly axial.
- For the case of oblique nozzles, the cracks are likely to be skewed axial cracks, oriented in a direction 90° to that of the maximum principal stress, and centered on the uphill and downhill sides of the nozzles.
- It should be assumed that all Alloy 600 nozzles attached to vessel shells by J-groove welds have operating condition stresses high enough to cause PWSCC unless it can be shown by analysis, or other means, that the stresses are below a stress threshold of about 250 MPa.

8. ACKNOWLEDGMENTS

The work described in this paper was sponsored by several organizations. Particular thanks go to EPRI, the Combustion Engineering Owners Group, Duke Power, New York Power Authority and Rochester Gas & Electric.

9. REFERENCES

1. PWSCC of Alloy 600 Materials in PWR Primary System Penetrations. April 1994. EPRI TR-103696.

2. M. H. Duc. "Specification de Calcul de Maquettes d'adaptateurs." EdF Specification ENT-MS-92-090-A CPE: A667M.

3. Proceedings: 1991 EPRI Workshop on PWSCC of Alloy 600 in PWRs. December 1990. EPRI NP-7094.

4. Proceedings: 1992 EPRI Workshop on PWSCC of Alloy 600 in PWRs. July 1992. EPRI TR-100852.

5. Residual Stress Measurements on Alloy 600 Pressurizer and Heater Sleeve Mockups. December 1993. EPRI TR-103104.

6. B. Wilson. "Inspection and Repair Strategy for Reactor Vessel Head Penetrations in Ringhals. Proceedings: 1992 EPRI Workshop on PWSCC of Alloy 600 in PWRs. July 1992. EPRI TR-100852.